UCRL-JC-119645

CONF-9506352--2

Sources of Optical Distortion in Rapidly Grown Crystals of KH_2PO_4

J. J. De Yoreo, Z. U. Rek, N. P. Zaitseva,
B. W. Woods, and T. A. Land

This paper was prepared for submittal to the
International Conference on Crystal Growth XI
The Hague, Netherlands
June 18-23, 1995

March 20, 1995

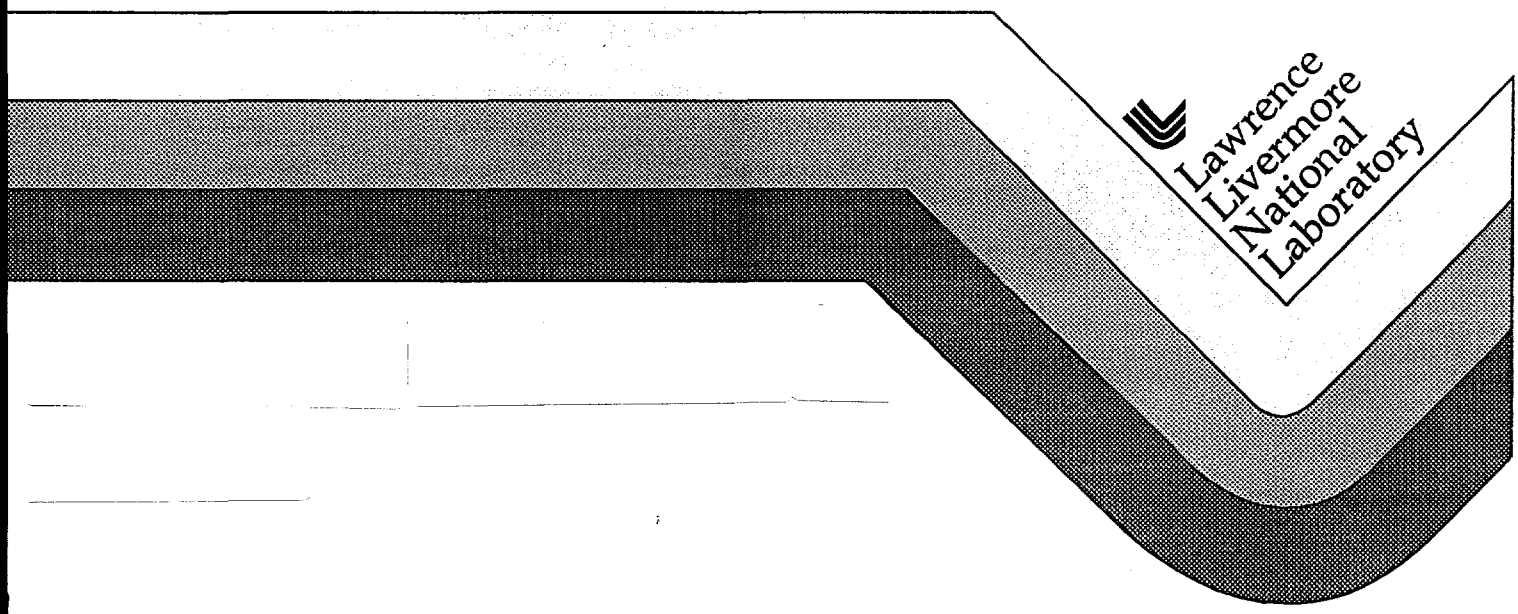

Sources of optical distortion in rapidly grown crystals of KH_2PO_4

J. J. De Yoreo, Z.U. Rek*, N.P. Zaitseva, B.W. Woods and T.A. Land

Lawrence Livermore National Laboratory, Livermore, CA 94550
*Stanford Synchrotron Research Laboratory, Stanford, CA 94309

Abstract

We report the results of X-ray topographic and optical measurements on KH_2PO_4 crystals grown at rates of 5 to 30mm/day. We show that optical distortion in these crystals is caused primarily by three sources: dislocations, differences in composition between adjacent growth sectors of the crystal and differences in composition between adjacent sectors of vicinal growth hillocks within a single growth sector of the crystal. We find that the compositional heterogeneities cause spatial variations in the refractive index and induce distortion of the transmitted wave front while large groups of dislocations are responsible for strain induced birefringence which leads to beam depolarization.

Introduction

Due to their interesting electrical and optical properties, structural phase transitions, and ease of crystallization, KH_2PO_4 (KDP) and its isomorphs have been the subject of a wide variety of investigations for over 40 years[1,2]. Today, KDP and its deuterated analog, KD_2PO_4 (DKDP), are widely used to control the parameters of laser light such as pulse length, polarization and frequency through the first and second order electro-optic effects[3,4].

Efficient operation of electro-optic devices such as Pockels cells and frequency converters requires crystals with a high degree of perfection. In particular, internal strains in the crystals generate spatial variations in the refractive index tensor through the stress-optic effect.[5] While these phenomena are a minor issue for the small crystals typically used in laboratory research applications, the effect of strain is the limiting factor on performance in applications requiring large aperture crystals such as inertial confinement fusion[6] and high average power laser systems.[7] De Yoreo et al.[8] analyzed the effect of internal stresses on the refractive index tensor and quantitatively related the magnitude of the stresses to experimentally determined variations in the transmitted wave front and beam polarization in KDP and DKDP crystals grown by conventional techniques. Recently, Zaitseva et al.[9] described a method for growing bulk single-crystals of KDP from solutions at high supersaturation which produces growth rates of 5 to 30mm/day or ten to fifty times those obtained with conventional methods. The purpose of this paper is to describe the results of X-ray topographic and optical measurements on KDP crystals grown by this technique. We show that optical distorion in these crystals is caused primarily by three sources: dislocations, differences in composition between adjacent growth sectors of the crystal and variations in composition between adjacent

sectors of vicinal growth hillocks within a single growth sector of the crystal. We find that the compositional heterogeneities cause variations in the refractive index and induce distortion of the transmitted wave front while large groups of dislocations are responsible for strain induced birefringence which leads to beam depolarization.

Experimental Methods

Crystals of KDP were grown from high purity starting materials by the method of temperature reduction[9] at growth rates of 5 to 30 mm/day along the <001> direction. Above 10mm/day, the growth rate along the {100} directions was comparable to that along <001>. However, at 5mm/day, the rate along {100} was generally ≤ 2mm/day and varied by more than a factor of two. The samples used in this study were 1cm thick plates oriented with the plate normal along <001> and were cut from the entire cross section of the boule. The surfaces were prepared by single point diamond turning which gave excellent surfaces for both the optical and X-ray topographic experiments.

Two measurements of optical distortion were performed in order to determine the spatial distribution of the optic index as well as the magnitude of the anomalous birefringence. The distortion of the transmitted wave front was measured using a commercial interferometer. This technique measures the spatial variation of the phase, Γ, which is related to the index of refraction, n, by:[8]

$$\Gamma = \frac{2\pi}{\lambda} (n-n_o)\, l \qquad (1)$$

where λ is the wavelength, n_o is the ordinary index and l is the thickness of the crystal.

The anomalous birefringence was measured using a circular polarimeter as described previously.[8] This technique determines the degree of depolarization induced by the crystal which is measured as a loss in the intensity, L, of the portion of beam polarized along the direction of the input polarization. L is related to the birefringence, δn, by the relationship:[8]

$$L = \sin^2(\pi \delta n l/\lambda) \qquad (2)$$

(In addition to providing a measure of index inhomogeneities, operationally, Γ and L are the two quantities which determine the quality of KDP crystals to be used in laser systems as Q-switches and frequency converters.)

X-ray topographs were collected in reflection using white beam synchrotron radiation at Stanford Synchrotron Research Laboratory. The nominal beam size was 20x30mm and the beam was filtered through Mo foil before incidence on the crystal. By translating the crystal along the <100> and <010> directions, a composite image of the entire crystal was produced. The images shown in this paper are asymmetric reflections collected with the crystal and detector normals tilted at 80° and 70° respectively to the beam direction. The image aspect ratios have been adjusted to reflect the true aspect ratio of the crystal.

Results and discussion

Single crystal boules of KDP grown at high supersaturation advance on both the {101} (pyramidal) and {100} (prismatic) facets of the crystal leading to a pyramidal

crystal habit as shown schematically in Figure 1a. Advance of the crystal face on both sets of facets occurs on steps generated at vicinal growth hillocks formed by dislocations emanating either from the seed (see Figure 1a and c) or from foreign inclusions incorporated during growth.[1,10,11] As the AFM image in Fig.1 shows, the vicinal hillocks on the {101} face have an asymmetric triangular pyramidal geometry. Figure 1c is an AFM image of the top of a growth hillock on the {101} face showing that the steps are generated by a group of dislocations with a net Burgers vector of five unit steps. Each step is 5Å in height which is half the unit cell dimension in the {101} direction and corresponds to one monomolecular layer, i.e. the distance between K-planes. The sectors of the vicinal hillock with the shallowest (sector 3) and steepest (sector 1) slopes generate steps oriented roughly along the pyramid-pyramid and pyramid-prism boundaries respectively. Both the triangular shape of the hillocks and the slope asymmetries have been attributed to anisotropy in the adsorption and diffusion kinetics.[10,12] As Fig. 1c shows, the dislocations themselves generate hollow cores when the Burgers vector is greater than one unit step due to the effect of strain on crystal stability.[10,13,14]

In general, crystals cut from the full cross section of a boule contain eight different growth sectors corresponding to the eight {101} and {100} directions as shown in Fig. 1d. Within the individual {101} sectors, lie sub-boundaries corresponding to the division between the three sectors of the vicinal hillocks (vicinal sector boundaries) as well as the boundaries between adjacent vicinal hillocks (intervicinal boundaries).[15] Dislocations within the {101} sectors typically run at a steep angle to the surface while those in the {100} sectors lie nearly in the plane of the crystal surface.[16]

Figure 2a shows a composite of X-ray topographs of a 8.8x7.6cm KDP crystal cut from the central portion of a boule grown at 5mm/day along the <001> axis. The {101}-{101} boundaries are faintly visible and there is pronounced contrast between the {101} and the {100} sectors. This contrast is also seen in the transmitted wave front profile in Figure 2b, showing that it is correlated with a variation in the optic index of refraction of the crystal, a reflection of its composition. The depolarization loss profile (not shown) has a similar pattern with little birefringence in the pyramidal sectors and high loss in the prism sectors. We conclude that, at low growth rates along {100}, impurities are preferentially incorporated on the {100} faces in agreement with the results of previous investigators[17] obtained on crystals grown at much lower growth rates (~1mm/day) along <001>.

Figure 3 shows a composite of X-ray topographs of a portion of a 11.5x10.0cm KDP crystal cut from the upper portion of a boule grown at 13mm/day along <001>. There are three main features to this topograph: pyramid-pyramid sector boundaries (S), numerous groups of dislocations (D) and a set of domain-like structures with rectilinear boundaries which correspond to vicinal sector boundaries (V) and intervicinal boundaries (I). The shallowest sector exhibits the highest contrast relative to the other two sectors showing that its lattice parameters are the most dissimilar. Smolskii et al.[15] suggested that the contrast was due to variations in impurity content caused by differences in the segregation coefficient for the three step directions. Figure 4 shows the effect of these defects on the anomalous birefringence of crystals cut from three locations in the boule. While the sector boundaries are clearly visible in this profiles, vicinal sectorality leaves little or no signature and only the groups of

dislocations with the strongest contrast cause significant levels of beam depolarization.

Figure 5a shows a composite of X-ray topographs of an 8.5x7.5cm crystal cut from the upper portion of a boule grown at 30mm/day along <001>. At this high growth rate, the vicinal sectorality is strongly pronounced. The effect of this type of defect on the optic index is illustrated in Fig. 5b which shows a static fringe interferogram of the crystal in Fig. 5a. Comparison of the two figures shows that the breaks and distortions in the fringes coincide with the locations of vicinal and intervicinal sector boundaries. These results demonstrate that vicinal sectorality is strongly correlated with variations in optic index of refraction and supports the hypothesis that the contrast in the topographs is caused by differences in impurity content between adjacent vicinal sectors.

One of the striking features of these results is that the degree of compositional difference between the {100} and {101} sectors decreases with increasing growth rate while the variations between the vicinal sectors within the {101} sectors increases. The latter effect can be understood if the contrast in composition is due to a difference in segregation coefficient for the three step directions as mentioned above. As growth proceeds, a diffusion profile for impurities with a peak at the crystal surface develops in the poorly mixed region immediately adjacent to the crystal. The impurity level in the crystal is determined by both the segregation coefficient and the the height of the peak in this diffusion profile. As the growth rate increases, the diffusion profile for rejected impurities should become steeper and the absolute difference between impurity levels in adjacent sectors will be an increasing function of both the difference in segregation coefficient and the growth rate. The reduction of compositional

contrast between {100} and {101} sectors with increasing growth rate can not be explained in the same fashion. In fact, this result suggests that impurities are less likely to become incorporated into the prism faces as the growth rate increases, contrary to the expected behavior.

Conclusion

The results presented here show that optical distortion from KDP crystals can be related to defects visible with X-ray topography which are fundamentally connected to the growth mechanism. Strong bundles of dislocations cause high levels of strain induced birefringence while differences in composition between adjacent sectors of the crystal as well as vicinal hillocks on the faces of the growing crystal generate variations in the optic index of refraction.

Acknowledgements

This work was performed under the auspices of the Division of Material Sciences, US Department of Energy and Lawrence Livermore National Laboratory under Contract No. W-7405-ENG-48.

References

1. For a review on KDP crystal growth see: Rashkovich, L.N., *KDP Family Single Crystals* (Adam Hilger, New York, 1991).
2. For a review on KDP structure, properties and applications see:Ferroelectrics, **71** and **72**, (1987).
3. Zernicke, F. and Midwinter, J.E., *Applied Non-inear Optics* (John Wiley & Sons, New York, 1973).
4. Eimerl, D., Ferroelectrics, **72**, 95 (1987).
5. Nye, J. F., *Physical properties of crystals*, ch. 13 (Oxford University Press,New York, 1985).
6. J.J. De Yoreo, and B.W. Woods, in: *Inorganic crystals for optics, electro-optics and frequency conversion*, Proc. Int. Soc. Optic. Engin., SPIE,**1561**, P.F.Bordui, Ed. (SPIE, Bellingham, WA ,1991, p.50).
7. Eimerl, D., *I*EEE Journal of Quantum Electronics, **23**, 2238 (1987).
8. De Yoreo, J.J. and Woods, B.W., J. App. Phys. **73**, 7780 (1993).
9. N.P. Zaitseva, I.L. Smol'skii and L.N. Rashkovich, *Kristallografiya* **36**, 113 (1991).
10. J.J. De Yoreo, T.A. Land and B.J. Dair, *Phys. Rev. Lett.*, **73**, 838 (1994).
11. A.A. Chernov, I.L. Smol'skii, V.F. Parvov, Yu. G. Kuznetsov and V.N. Rozhanskii, *Sov. Phys. Crystallogr.* **25**, 469 (1980).
12. P.G. Vekilov, Yu.G. Kuznetsov and A.A. Chernov, *J. Cryst. Growth* **121**, 643 (1992).
13. F.C. Frank, *Acta Cryst.* **4**, 497 (1951).
14. N. Cabrera and M.M. Levine, *Phil. Mag.* **1**, 450 (1956).
15. I.L. Smol'skii, A.A. Chernov, Yu. G. Kuznetsov, V.F. Parvov, and V.N.

Pozhanskii, *Sov. Phys. Crystallogr.* **30**, 971 (1985).

16. H. Klapper, Yu. M. Fishman and V.G. Lutsau, *Phys. Stat. Sol. (a)* **21**, 115 (1974).
17. Belouet, C., Dunia, E. and Petroff, J.F., J. Cryst. Growth, **29**, 109 (1975).

Figures

Figure 1: (a) Illustration of the growth habit of a single crystal boule of KDP showing the location of the seed, dislocations and the geometry of vicinal growth hiilocks. (b) Location of sector boundaries in a plate of KDP cut perpendicular to the {001} axis. (c) 5.6x5.6μm AFM image of a hillock on the {101} face showing structure of step anisotropy. (d) 2.7x2.5μm AFM image of a complex dislocation source at the top of a hillock on the {101} face with a net Burgers vector of five unit steps showing hollow core when the Burgers vector exceeds one unit step.

Figure 2: (a) Composite white beam X-ray topograph and (b) transmitted wave front profile of an (001) plate of KDP with dimensions 8.8x7.6x1.0cm^3. **S**- crystal sector boundaries.

Figure 3: (a) Composite white beam X-ray topograph of a portion of the (001) plate of KDP shown in Fig. 3d with dimensions 11.5x10.0x1.0cm^3. **S**- crystal sector boundaries, **V**- vicinal sector boundaries, **I**- intervicinal boundaries, **D**- strong dislocation bunches, and **T**- tops of growth hillocks.

Figure 4: (a) Location of plates in (b) - (d) and depolarization profiles of plates cut from (b) just above the seed, (c) the middle of the boule and (d) just above the pyramidal cap. The topograph for the crystal in d is given in Fig. 3. Crystal sizes are 11.5x10.0x1.0cm^3.

Figure 5: (a) Composite white beam X-ray topograph and (b) static fringe interferogram of an (001) KDP plate with dimensions 8.5x7.5x1cm^3. In the

absence of bulk index inhomogeneities, the fringes would be straight and parallel. Symbols are as in Figure 3.

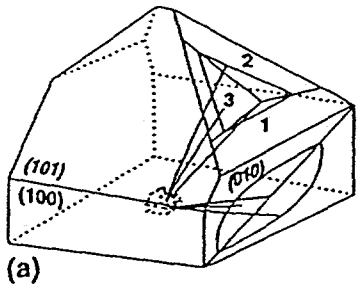

(a)

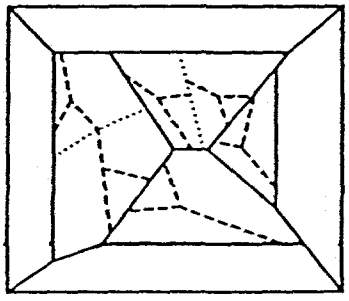

(b)

fig 1a and b

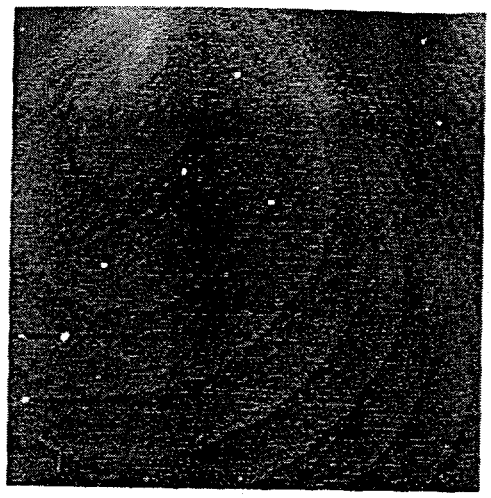

(c)

(d)

De Yoreo et al., Fig. 1c and d

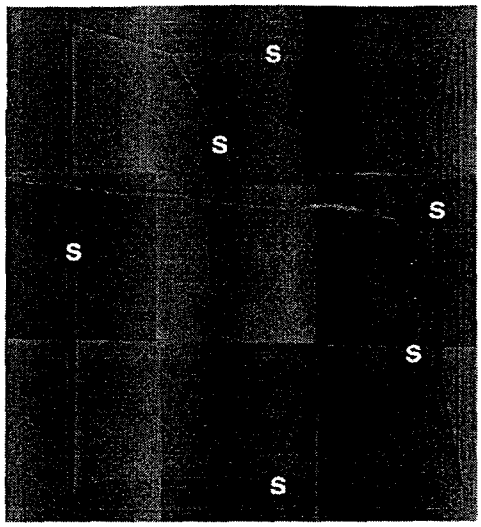

a

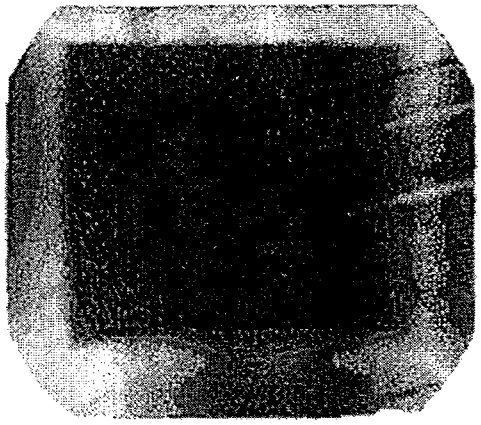

b

Fraction of a wavelength

-0.16 +0.18

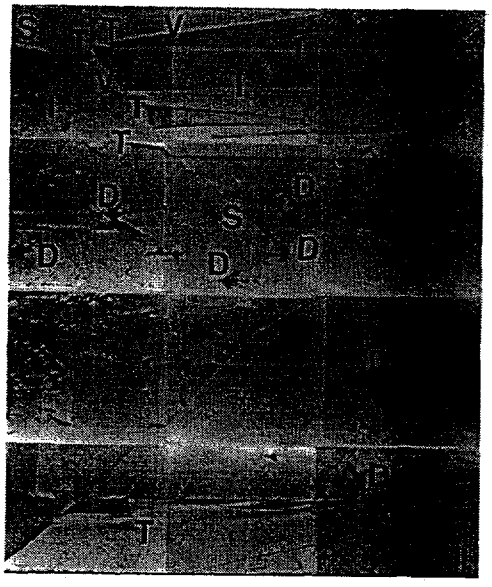

De Yoreo et al., Fig. 3

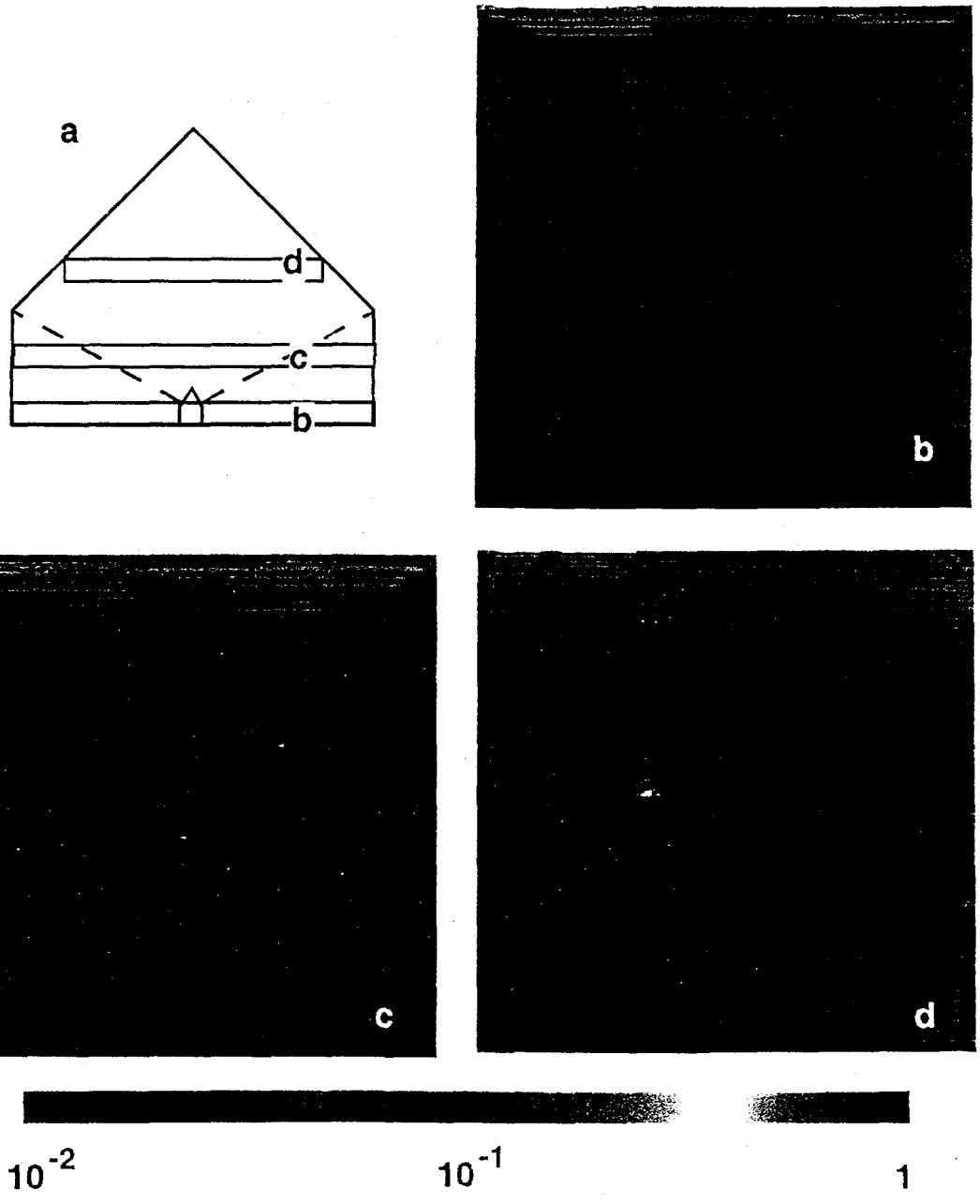

De Yoreo et al. Fig. 4

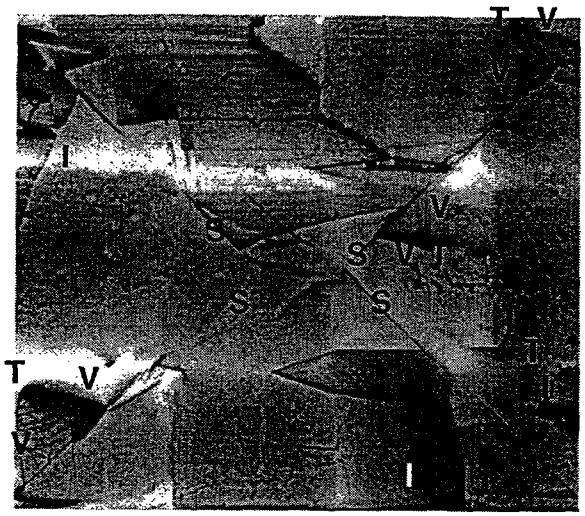

(a)

(b)

De Yoreo et al., Fig. 5a&b